fermentation

MDPI

Article

Molecular Characterization of a Stable and Robust L-Asparaginase from *Pseudomonas* sp. PCH199: Evaluation of Cytotoxicity and Acrylamide Mitigation Potential

Subhash Kumar [1,2,†], Sanyukta Darnal [1,2,†], Vijeta Patial [1,2], Virender Kumar [1] and Dharam Singh [1,2,*]

[1] Biotechnology Division, CSIR-Institute of Himalayan Bioresource Technology, Palampur 176061, Himachal Pradesh, India
[2] Academy of Scientific and Innovative Research (AcSIR), Ghaziabad 201002, India
* Correspondence: dharamsingh@ihbt.res.in or dharams14@gmail.com; Tel.: +91-1894-233339
† These authors contributed equally to this work.

Abstract: L-asparaginase is an important industrial enzyme widely used to treat acute lymphoblastic leukemia (ALL) and to reduce acrylamide formation in food products. In the current study, a stable and robust L-asparaginase from *Pseudomonas* sp. PCH199, with a high affinity for L-asparagine, was cloned and expressed in *Escherichia coli* BL21(DE3). Recombinant L-asparaginase (*Pg*-ASNase II) was purified with a monomer size of 37.0 kDa and a native size of 148.0 kDa. During characterization, *Pg*-ASNase II exhibited 75.8 ± 3.84 U/mg specific activities in 50.0 mM Tris-HCl buffer (pH 8.5) at 50 °C. However, it retained 80 and 70% enzyme activity at 37 °C and 50 °C after 60 min, respectively. The half-life and k_d values were 625.15 min and 1.10×10^{-3} min^{-1} at 37 °C. The kinetic constant K_m, V_{max}, k_{cat}, and k_{cat}/K_m values were 0.57 mM, 71.42 U/mg, 43.34 s^{-1}, and 77.90 ± 9.81 s^{-1} mM^{-1} for L-asparagine, respectively. In addition, the enzyme has shown stability in the presence of most metal ions and protein-modifying agents. *Pg*-ASNase II was cytotoxic towards the MCF-7 cell line (breast cancer) with an estimated IC_{50} value of 0.169 U/mL in 24 h. Further, *Pg*-ASNase II treatment led to a 70% acrylamide reduction in baked foods. These findings suggest the potential of *Pg*-ASNase II in therapeutics and the food industry.

Keywords: L-ASNase II; Himalayan bacteria; enzyme; cytotoxicity; acrylamide reduction

Citation: Kumar, S.; Darnal, S.; Patial, V.; Kumar, V.; Singh, D. Molecular Characterization of a Stable and Robust L-Asparaginase from *Pseudomonas* sp. PCH199: Evaluation of Cytotoxicity and Acrylamide Mitigation Potential. *Fermentation* **2022**, *8*, 568. https://doi.org/10.3390/fermentation8100568

Academic Editor: Xian Zhang

Received: 4 October 2022
Accepted: 20 October 2022
Published: 21 October 2022

1. Introduction

L-asparaginase (L-ASNase; EC 3.5.1.1) is a commercially important therapeutic enzyme. It is widely used in pharmaceuticals for the treatment of acute lymphoblastic leukemia (ALL) and in food industries for acrylamide mitigation, boosting interest in its extensive research [1]. Normal blood cells synthesize L-asparagine due to L-asparagine synthetase activity. In contrast, leukemic cells are devoid of L-asparagine synthetase activity, thus depending on external uptake of the amino acid for their growth and survival [2,3]. L-ASNase is obtained from various organisms, including bacteria, and can be classified into different types [4]. The L-ASNases from bacteria are of two types: type I (cytosolic) and type II (periplasmic) [5,6]. Type I has a lower, while type II has a higher affinity for the substrate L-asparagine [4].

The K_m value of L-ASNase must be in a lower micromolar range (~50 μM) for efficient hydrolysis of blood L-asparagine [6]. The hydrolytic capability of type II L-ASNase is utilized to treat ALL. It depletes the circulating blood plasma L-asparagine, resulting in the death of malignant lymphoblastic cells [7]. Besides treating ALL, L-ASNase is also explored in anticancer applications for lung and breast cancers [8,9]. L-ASNase II from *Escherichia coli* (*E. coli*) and *Dickeya chrysanthemi* (*D. chrysanthemi*) are currently used to treat

ALL. However, these formulations are associated with several adverse immunogenic effects, limiting their use as an exclusive therapeutic agent [10–12]. In addition, commercial L-ASNase also has L-ASNase-associated L-glutaminase (L-GLNase) activity.

L-ASNase is also used in the food industry for acrylamide mitigation [13]. When food is baked or fried at temperatures above 120 °C, it results in acrylamide formation, also known as the Maillard reaction [14]. Acrylamide is potentially neurotoxic, genotoxic, and carcinogenic to human health [15]. Commercially available L-ASNase for acrylamide mitigation is PreventAse® (DSM 2018) and Acrylaway® (Novozymes) [16]. Furthermore, there is no report of commercial bacterial L-ASNases for acrylamide mitigation. Because of its potential applications in food processing and medicine, L-ASNase demand is increasing several-fold. The bacterial L-ASNase with increased stability, high affinity for L-asparagine, lower L-GLNase activity, and a physiologically appropriate half-life are prerequisites for commercial application. Therefore, efforts are required to explore novel and unique sources of L-ASNases to fulfill the increasing medical and food industry demands.

Microbes thriving in high-altitude environments have unique characteristics such as low oxygen survival and tolerance to a wide range of pH, salt, temperature fluctuations, and UV radiations [17–19]. These extreme conditions allowed microbes to acquire peculiar and industrial-friendly robust features. Our laboratory is focused on bacterial L-ASNases from high-altitude niches that exhibit exceptional adaptability and robust substrate-specificity [20–22]. The present work explored the recombinant L-ASNase of the Himalayan *Pseudomonas* sp. PCH199 strain. The heterologous expression and molecular characterization of purified recombinant L-ASNase were performed. The current investigation revealed the recombinant L-ASNase, a potential chemotherapeutic agent with a high degree of cytotoxicity to cancer cells, along with acrylamide mitigation potential.

2. Materials and Methods

2.1. Chemicals, Bacterial Strains, and Cell Line

Taq DNA polymerase was purchased from NEB (Hitchin, UK). FastDigest endonucleases (*Nde*I, *Sac*II, and *Xho*I), T4 DNA Ligase, DNA ladder (1.0 kb), dNTPs, and HisPur Cobalt resin superflow were procured from Thermo Fisher Scientific (Waltham, MA, USA). Q-sepharose resin was obtained from GE Healthcare, Merck (Darmstadt, Germany). Precision Plus Protein™ Dual Color Standards protein marker was obtained from Biorad (Hercules, CA, USA). Plasmid and DNA (PCR/Gel) purification kits were obtained from Favorgen (Ping Tung, Taiwan). The expression vector pET-47b(+) and *E. coli* BL21(DE3) were purchased from Novagen (St. Louis, MO, USA). MCF-7 cell line was purchased from the National Centre for Cell Science (Pune, India). All other molecular biology-grade media components were obtained from Sigma-Aldrich (St. Louis, MO, USA) and Hi-Media (Mumbai, India).

2.2. Sequence Analysis and Cloning of Pg-asn II

The gene (*Pg-asn* II) encoding the type II L-ASNase enzyme (NCBI ID: OM621889) was retrieved from the whole-genome sequence of *Pseudomonas* sp. PCH199 (Project ID: PRJNA668072, Biosample ID: SAMN16396550). The nucleotide sequence was examined and translated using the ExPASy translate tool. The presence of signal peptide was determined using SignalP 5.0 [23]. The ProtParam tool was used to calculate the theoretical isoelectric points (pI) and molecular mass of L-ASNase. (https://web.expasy.org/protparam/, accessed on 3 October 2022). Subsequently, the protein sequence was compared to the L-ASNase database sequence in UniProt (https://www.uniprot.org/blast/, accessed on 3 October 2022). ClustalW (https://www.genome.jp/tools-bin/clustalw, accessed on 3 October 2022) and ESPript 3.0 were used to accomplish multiple sequence alignment [24]. The enzyme homology model was designed using the SWISS-MODEL server (https://swissmodel.expasy.org/, accessed on 3 October 2022).

Two sets of forward primers: with His-tags (F1) and tag-free (F2), were designed. The forward primers, F1 (5′-TCCCCGCGGCTATGAAAGAAGTCGAAACCCAGACC-3′) was flanked by *Sac*II and F2 (5′-GGGAATTCCATATGAAA-GAAGTCGAAACCCAGACCA-3′) was flanked by *Nde*I. The reverse primer (5′-CCGCTCGAGTCAGTATTCCCAGAA-3′) was flanked by *Xho*I and used to amplify both tagged and tag-free sequences. NetPrimer was used to examine the attributes such as T_m, cross dimer, ΔG, and self-dimer of the designed primers (Premier Biosoft, Palo Alto, CA, USA). The *Pg-asn* II gene was amplified using PCH199 genomic DNA. The PCR products were purified using a Gel/PCR purification kit (Favorgen, Ping Tung, Taiwan) and digested with *Sac*II-*Xho*I and *Nde-Xho*I, respectively. The purified PCR product was ligated using T4 DNA ligase into respective double-digested pET-47b(+) vector. The ligated product was transformed in *E. coli* BL21(DE3) using the standard heat-shock method [25]. The transformed cells were spread on Luria Bertani (LB) medium supplemented with Kanamycin (25.0 μg/mL) and incubated at 37 °C. The clones containing recombinant plasmids (pET-47b-*Pg-asn* II) were confirmed by colony PCR, and sequencing was performed using a vector-specific primer (T7 promoter and terminator). The sequences were analyzed using FinchTV 1.4 to obtain the consensus sequence.

2.3. Expression of Recombinant Pg-ASNase II

E. coli BL21(DE3) culture containing recombinant pET-47b-*Pg-asn* II plasmid was selected for the expression of *Pg*-ASNase II. The 50 mL LB-Kanamycin (25.0 μg/mL) media in a 250 mL flask was inoculated with recombinant colonies and checked for expression at 37 °C and 200 RPM. The expression of *Pg*-ASNase II was obtained by inducing the culture with 0.5 mM IPTG and incubating it at 37 °C for 20 h. After incubation, the culture was centrifuged at 8000× *g* for 20 min to recover the cell pellet. Further, the pellet was thoroughly washed with 50.0 mM Tris-HCl buffer (pH 8.5) to remove residual media traces. The cell pellet was dissolved in Tris-HCl buffer and checked for a specific activity, total protein content, and expression in SDS-PAGE.

2.4. Production Parameter Optimization

Various production parameters were selected to optimize the maximum production of *Pg*-ASNase II. The concentration of IPTG (0.1, 0.3, 0.5, 0.7, and 1.0 mM), incubation temperature (20, 28, and 37 °C), stage of induction (0.4–2.4 OD), agitation (150, 200, 250, and 300 RPM), and time course (0–30 h) after induction were optimized for maximum expression of *Pg*-ASNase II. Similar studies were also carried out for *Pg*-ASNase II having no His-tag moiety.

2.5. Purification of Recombinant Pg-ASNase II

After optimum production, the bacterial culture was centrifuged at 8500× *g* for 15 min and washed thoroughly with Tris-HCl buffer to remove residual media traces. The *Pg*-ASNase II with His-tag moiety was dissolved in basic buffer (50.0 mM Tris-HCl, 300.0 mM NaCl, and 5.0 mM Imidazole), and the one without His-tag was resuspended in Tris-HCl buffer (25.0 mM; pH 8.2), respectively. The cell suspension was sonicated for 30–35 min on ice and centrifuged (8000× *g* for 25 min) to obtain the supernatant, a cell-free extract. Purification of *Pg*-ASNase II was performed using affinity (HisPur Cobalt Superflow) and anion exchange chromatography (Q-Sepharose FPLC) depending upon the presence or absence of His-tag moiety, respectively. The cell-free extract was loaded onto the chromatography columns equilibrated with their respective buffers. In the case of HisPur Cobalt Super-flow chromatography, the bound *P*g-ASNase II was eluted using elution buffer (50.0 mM Tris-HCl pH 8.5, 300.0 mM NaCl, and 150.0 mM imidazole) in different fractions. The bound recombinant protein was eluted through anion exchange chromatography using 1.0 M NaCl prepared in 25.0 mM Tris-HCl buffer at different gradients. The purified fractions of *Pg*-ASNase II with and without His-tag were pooled separately

and dialyzed with Tris-HCl buffer. The purity of the *Pg*-ASNase II was determined using SDS-PAGE [26], and native conformation was determined by gel exclusion chromatography (Superdex 200, GE Healthcare, Chicago, IL, USA). The native molecular weight was calculated using different molecular weight standards (Merck-Sigma Aldrich, St. Louis, MO, USA).

2.6. Pg-ASNase II Activity

The activity of *Pg*-ASNase II was measured spectrophotometrically at 480 nm using Nessler's reagent. It measures the amount of ammonia released after the hydrolysis of L-asparagine in a reaction mixture [20,27]. Briefly, the L-ASNase assay was carried out in a 1.0 mL volume of a reaction containing 0.48 mL Tris-HCl (50.0 mM, pH 8.5), 0.5 mL L-asparagine (10 mM prepared in Tris-HCl buffer), and 0.5 µg (0.02 mL) of *Pg*-ASNase II (enzyme suspended in Tris-HCl buffer). The reaction was incubated at 37 °C for 15 min and terminated by adding 0.25 mL of 1.5 M Trichloroacetic acid (TCA). For the control reaction, an enzyme was added after adding TCA. The reaction was diluted as per necessity before adding Nessler's reagent, and the absorbance was measured at 480 nm. The enzyme assay was performed in triplicate. The specific activity of purified *P*g-ASNase II was measured in U/mg protein (micromoles/min/mg). One unit (U) is described as the amount of *P*g-ASNase II liberating 1.0 µmol of ammonia per min under standard assay conditions.

2.7. Biochemical Characteristics of Pg-ASNase II

Various biochemical parameters for maximum *Pg*-ASNase II activity were optimized. The effect of buffer pH on *Pg*-ASNase II activity was investigated in the pH range of 4.0–13.0. The buffers (50.0 mM), viz. sodium citrate (pH 4–6), potassium phosphate (pH 6–8), Tris-HCl (pH 8–9.5), Glycine-NaOH (pH 9–10.5), sodium-bicarbonate (pH 10–11), and KCl-NaOH (pH 12–13) were used to obtain the optimum activity. The effect of buffer molarity (0.001 M to 1.0 M) on *Pg*-ASNase II activity was also measured. The optimum temperature range of *Pg*-ASNase II activity was estimated by performing the enzyme activity at different temperatures ranging from 4–70 °C. The optimum reaction time for maximum *Pg*-ASNase II activity was measured by incubating an enzyme-substrate reaction mixture ranging from 5–60 min at 37 °C. The enzyme concentration ranging from 0.1 to 5.0 µg in 1.0 mL reaction volume was used to optimize the enzyme concentration under standard assay conditions.

2.7.1. Thermal Stability of *Pg*-ASNase II

The thermostability of the purified *Pg*-ASNase II was evaluated by estimating the residual activity after incubating the enzyme in a wide range of temperatures (37, 50, 60, 70, and 80 °C). The enzyme activity was analyzed at different time intervals ranging from 5–90 min.

Evaluation of Deactivation Constant (k_d) and Half-life Time ($t_{1/2}$)

The k_d and $t_{1/2}$ were observed for *Pg*-ASNase II using the Arrhenius equation:

$$t_{1/2} = \ln 2/k_d = 0.693/k_d \quad (1)$$

where k_d is the deactivation rate constant.

2.7.2. Effect of Metal Ions, Detergents, and Protein Modifying Agents

The effect of metal ions, chelating agents, and detergents on *Pg*-ASNase II activity was evaluated. The *Pg*-ASNase II was pre-incubated with 1.0 mM $CuCl_2$, $ZnSO_4$, KCl, $CoCl_2$, $CaCl_2$, NaCl, and 2.0% sodium dodecyl sulfate (SDS), Tween 20, Tween 80, and Triton X-100. Similarly, protein modifying agents such as ethylenediaminetetraacetic acid

(EDTA), 2-mercaptoethanol (β-ME), phenylmethylsulfonyl fluoride (PMSF), and dithiothreitol (DTT) at 0.5, 1.0, and 2.5 mM were used to check the effect on *Pg*-ASNase II activity. The relative activity of the enzyme was considered in comparison to the control, i.e., the enzyme incubated without metal ions.

2.7.3. Determination of Kinetic Parameters: K_m, V_{max}, k_{cat}, and k_{cat}/K_m

The specificity of *Pg*-ASNase II for L-asparagine was measured using the substrate at different concentration ranges from 0.05–5.0 mM. The kinetic parameter such as K_m and V_{max} were calculated using the Michaelis-Menten equation and plotting 1/[s] and 1/[v] values in the Lineweaver-Burk plot. The turnover number (k_{cat}) of *Pg*-ASNase II was calculated by using the equation $k_{cat} = V_{max}/ [E_0]$, where $[E_o]$ is the initial *Pg*-ASNase II concentration in the assay and V_{max} (μmol/min) is the maximum reaction rate.

2.8. Cytotoxicity Effect of Pg-ASNase II on Cancer Cell Line

MCF-7 cells (breast cancer) were cultivated and maintained in a CO_2 incubator (37 °C, 98% humidity) in Dulbecco's modified Eagle's (DMEM) media supplemented with fetal bovine serum (10%), penicillin (100.0 U/mL), and streptomycin (100.0 g/mL). Cells were treated with varying enzyme doses for 24 h in the exponential phase, with Vinblastine as a positive control. The cytotoxic effect of the purified enzyme was assessed using the MTT [3-(4,5-dimethyl-2-thiazolyl)-2,5-diphenyl-2-tetrazolium bromide] test.

2.9. Estimation of Acrylamide Mitigation in the Potato Chips

Potatoes were purchased from the local market of Palampur, Himachal Pradesh, India. The potatoes were washed, skinned, and sliced into 2.0 ± 0.2 mm thick slices. Further, the potatoes were washed in distilled water to remove the adhering starch. To remove the excess water from the surface of the potato slices, they were dried in the oven at 40 °C for 20 min prior to treatment. Before frying, the potato slices (5.0 g) were pre-treated for 30 min in enzyme solution with concentrations of 1.0, 2.5, 5.0, and 10.0 U/mL at 37 °C. Similarly, the raw potato slices immersed in distilled water but not treated with enzymes were used as a control. The samples were fried in sunflower oil for 5 min at 180 °C. The fried samples were cooled to room temperature before extraction. The acrylamide content of the fried samples was analyzed by using Paleologos and Kontominas method with minor modifications [28].

3. Results

3.1. Sequence Analysis, Cloning, and Expression of Pg-ASNase II

The *Pg-asn* II gene of *Pseudomonas* sp. PCH199 was selected for cloning and expression due to its high L-ASNase activity without L-GLNase in wild-type compared to other screened bacterial isolates. The gene encoding for *Pg-asn* II, a type II L-ASNase enzyme, was obtained from the whole-genome sequence of *Pseudomonas* sp. PCH199. The signalP 5.0 server detected the presence of signal peptide in IMF27_28540, indicating periplasmic localization. Also, the theoretical pI was determined to be 6.25 for periplasmic L-ASNase using ProtParam. BLASTp analysis of *Pg*-ASNase II showed 93.4% similarity to L-ASNase of *Pseudomonas fluorescens* bv. A (*P. fluorescens*) (O68897.1). The protein-based phylogenetic analysis also showed clade formation and relatedness with the *P. fluorescens* L-ASNase gene (*Pg-asn* II) encoding the type II L-ASNase enzyme (NCBI ID: OM621889) was retrieved from the whole-genome sequence of *Pseudomonas* sp. PCH199 (Figure S1). Furthermore, the percent identity of *Pg*-ASNase II was 88.13% with *Pseudomonas putida* KT2440 (*P. putida*) (Q88K39.1), 63.64% with *Acinetobacter glutaminasificans* (*A. glutaminasificans*) (P10172.1), 47.58% with *E. coli* K-12 (P00805.2), and 45.92% with *E. chrysanthemi* (P06608.1) (Table S1). The two structural signature sequences, IlATGGTIA and GiVITHGTDTl, were recognized in *Pg*-ASNase II compared to selected L-ASNase sequences (Figure 1). The predicted active sites were Thr21 and Thr101 in *Pg*-ASNase II.

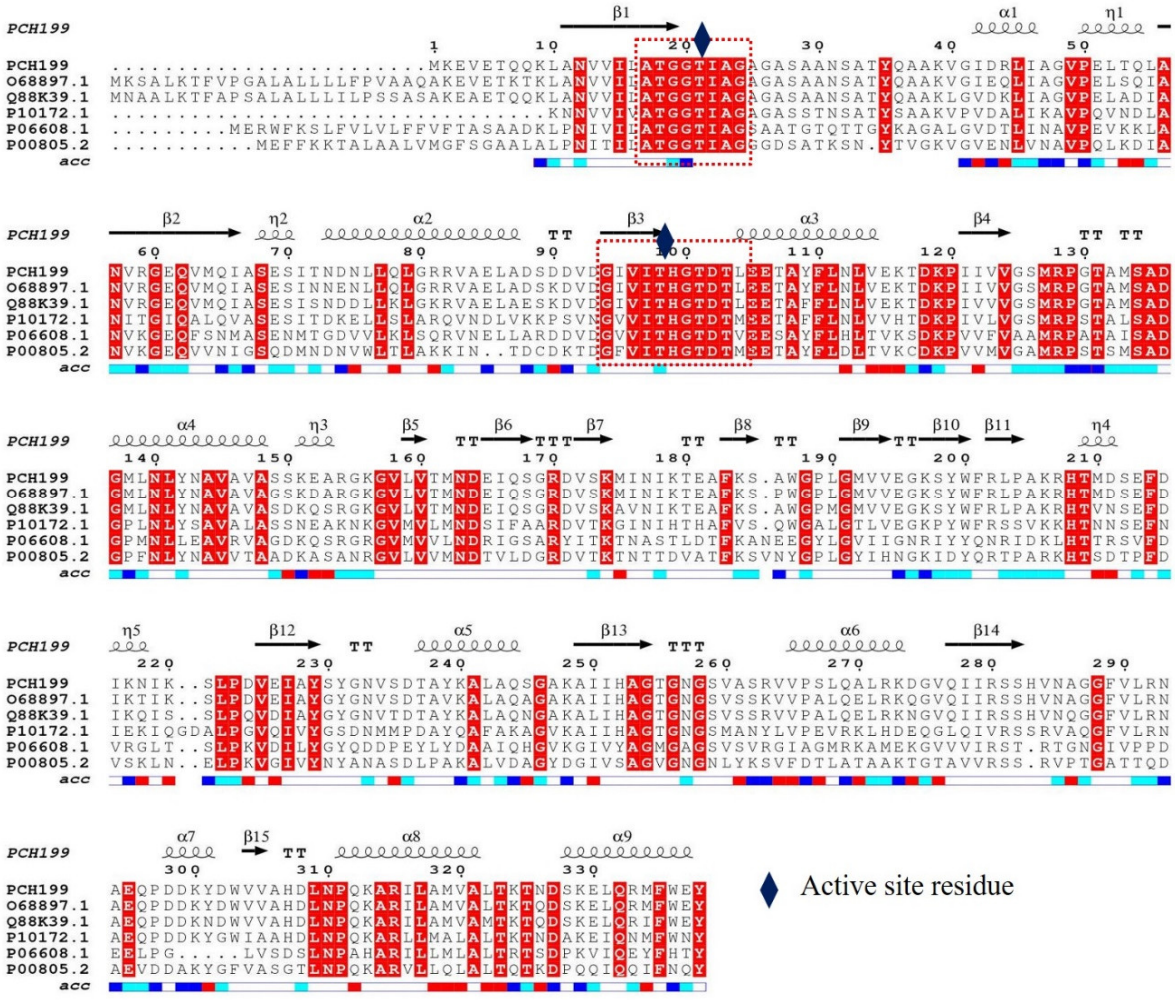

Figure 1. Multiple sequence alignment of *Pg*-ASNase II sequences using UniProt identifiers. Alignment of L-ASNases was performed by using ClustalW and ESPript 3.0. 'α' represents α-helix; 'β' represents β-sheet; 'η' represents 3_{10} helix; 'TT' represents strict β-turn; and 'TTT' represents strict α-turn. The secondary structure was observed from the 3D structure of *Pseudomonas* 7A glutaminase-asparaginase (PDB ID: 3PGA) and reported at the top.

A 1014 bases (without signal sequence) *Pg-asn* II gene of *Pseudomonas* sp. PCH199 was amplified with gene-specific primers. The amplified *Pg-asn* II was cloned in a pET-47b(+) expression vector with and without a His-tag moiety at the N-terminus. Further, the cloned sequence was confirmed by sequencing that validated the insert with a complete open reading frame. The positive clones were cultured in LB media and induced with 0.5 mM IPTG to express the heterologous protein. All selected recombinant colonies showed comparatively similar enzyme activity of 2.62 ± 0.02 U/mL after 6 h of induction (Figure S2).

3.2. Production Parameter Optimization

The production parameters of the cloned and expressed recombinant *Pg*-ASNase II were optimized. The highest *Pg*-ASNase II activity (his-tagged) was recorded at 2.77 ± 0.32 U/mL (considered 100%) after 6 h of induction using 0.3 mM IPTG. At 0.1 and 0.5 mM IPTG, no significant decrease was observed in *Pg*-ASNase II activity. However, at 0.7 and 1.0 mM concentrations, the enzyme activity dropped to 70.5 ± 2.0% (Figure S3). The maximum *Pg*-ASNase II activity of 2.82 ± 0.33 U/mL was observed at 37 °C after 10 h incubation (Figure S4A). The aeration condition was optimized and observed 2.88 ± 0.12 and 3.17 ± 0.04 U/mL *Pg*-ASNase II activities at 200 and 250 RPM, respectively (Figure S4B). At 250

RPM, froth formation might hinder enzyme activity, protein stability, and bacterial growth; therefore, 200 RPM was further selected for *Pg*-ASNase II production. The maximum *Pg*-ASNase II expression (3.19 ± 0.177 U/mL) was achieved at 1.2 OD_{600nm} after 20 h of induction (Figure S4C). Additionally, the optimum production time of 16 h after induction obtained a maximum activity of 3.63 U/mL (Figure S4D). Similarly, the production parameters were optimized for tag-free *Pg*-ASNase II. The maximum expression of 5.3 U/mL was achieved using 0.3 mM IPTG at 37 °C and 200 RPM after 10 h of incubation (Figure S5a–c). The optimized conditions were used for the maximum expression of *Pg*-ASNase II, followed by purification.

3.3. Purification of Pg-ASNase II

After expression, the *Pg*-ASNase II was purified from the soluble fraction using His-Pur Cobalt Super-Flow Agarose column and anion exchange chromatography depending upon the presence or absence of His-tag, respectively. The *Pg*-ASNase II purification using HisPur Cobalt Super-Flow Agarose column and anion exchange chromatography resulted in a final 83 and 86.7% yield with 20 and 14.67-fold purification, respectively (Table 1A,B). *Pg*-ASNase II was obtained as a single distinct band of 37.0 kDa on SDS-PAGE analysis (Figures 2A and S6). The native molecular weight was estimated at 148.0 kDa, revealing the tetrameric form of *Pg*-ASNase II (Figure 2B).

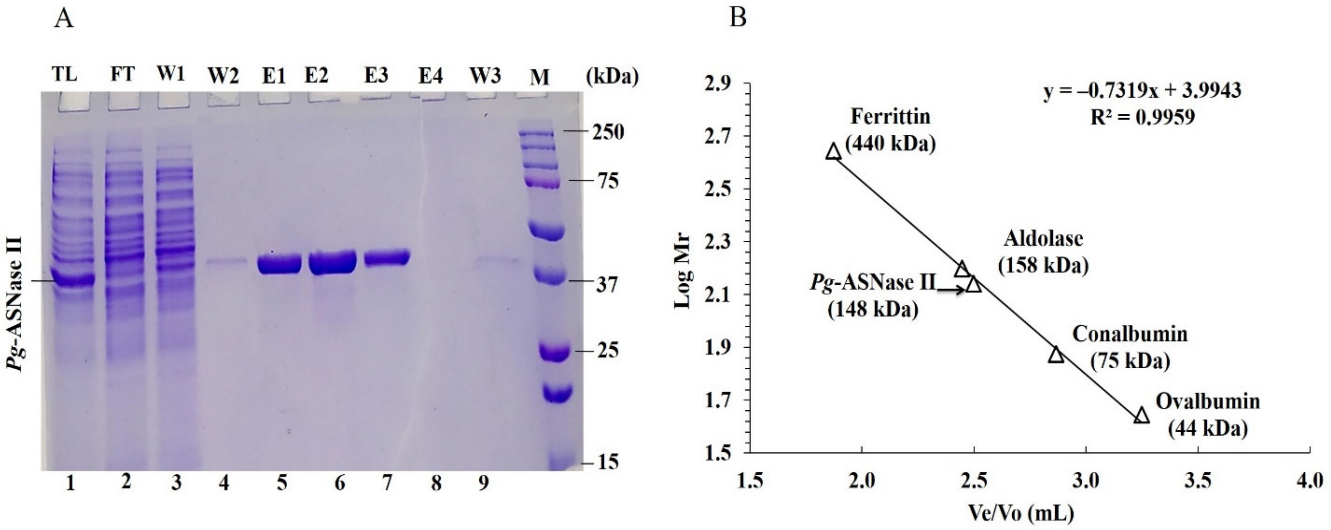

Figure 2. Polyacrylamide gel electrophoresis and molecular weight estimation of His–tagged *Pg*-ASNase II. (**A**) SDS–PAGE (12%) analysis of recombinant *Pg*-ASNase II. Lane 1 is total cell lysate; lane 2 is flow–through; lane 3 is a wash (W1) with 5.0 mM imidazole; lane 4 is a wash (W2) with 20.0 mM imidazole; lane 5–8 is eluted protein (E1–E4); lane 9 is a final wash (W3) with 250.0 mM imidazole, and M is protein molecular weight marker. (**B**) Determination of the molecular mass of the native *Pg*-ASNase II. Gel filtration chromatography was performed using Superdex 200 (10/300 GL) column. Arrow indicates the log MW of the *Pg*-ASNase II. Ferritin, aldolase, conalbumin, and ovalbumin were used as protein molecular weight standards for standard curves. V_e and V_o indicate for elution volume of each protein and void volume, respectively.

Table 1. Single-step purification for *Pg*-ASNase II. (A) Purification of His-tagged *Pg*-ASNase II using HisPur Cobalt resin column. (B) Purification of His-tagged free *Pg*-ASNase II using Q-Sepharose column.

A						
	Volume (mL)	**Total Protein (mg)**	**Specific Activity (U/mg)**	**Total Activity (U)**	**Purification Fold**	**Yield (%)**
Crude	10.0	10.0	3.00	30.0	1.0	100
His-tag affinity	1.2	0.42	59.22	25.0	20.0	83.0
B						
	Volume (mL)	**Total Protein (mg)**	**Specific Activity (U/mg)**	**Total Activity (U)**	**Purification Fold**	**Yield (%)**
Crude	140	495.6	3.28	1625.56	1.0	100
Q-Sepharose	2.0	29.3	48.12	1409.91	14.67	86.73

3.4. Effect of Different Reaction Parameters on Enzyme Activity

The his-tagged purified *Pg*-ASNase II was further used for the characterization. *Pg*-ASNase II exhibited activity across pH ranging from 4.0–12.0. The enzyme's maximum activity of 61.1 ± 4.0 U/mg was observed in Tris-HCl buffer at pH 8.5 (Figure 3A,B). *Pg*-ASNase II was active over a wide range of buffer molarity up to 700 mM, followed by a rapid reduction in *Pg*-ASNase II activity (Figure 3C). Maximum specific activity was achieved for an optimum amount of 0.5 µg/mL *Pg*-ASNase II (Figure 3D). On a range of 4 to 70 °C, the maximum *Pg*-ASNase II activity of 75.8 ± 3.84 U/mg was observed at 50 °C (Figure 3E). The *Pg*-ASNase II was stable at 4 °C for 28 days and at 22 °C for 5 days (Figure 3F).

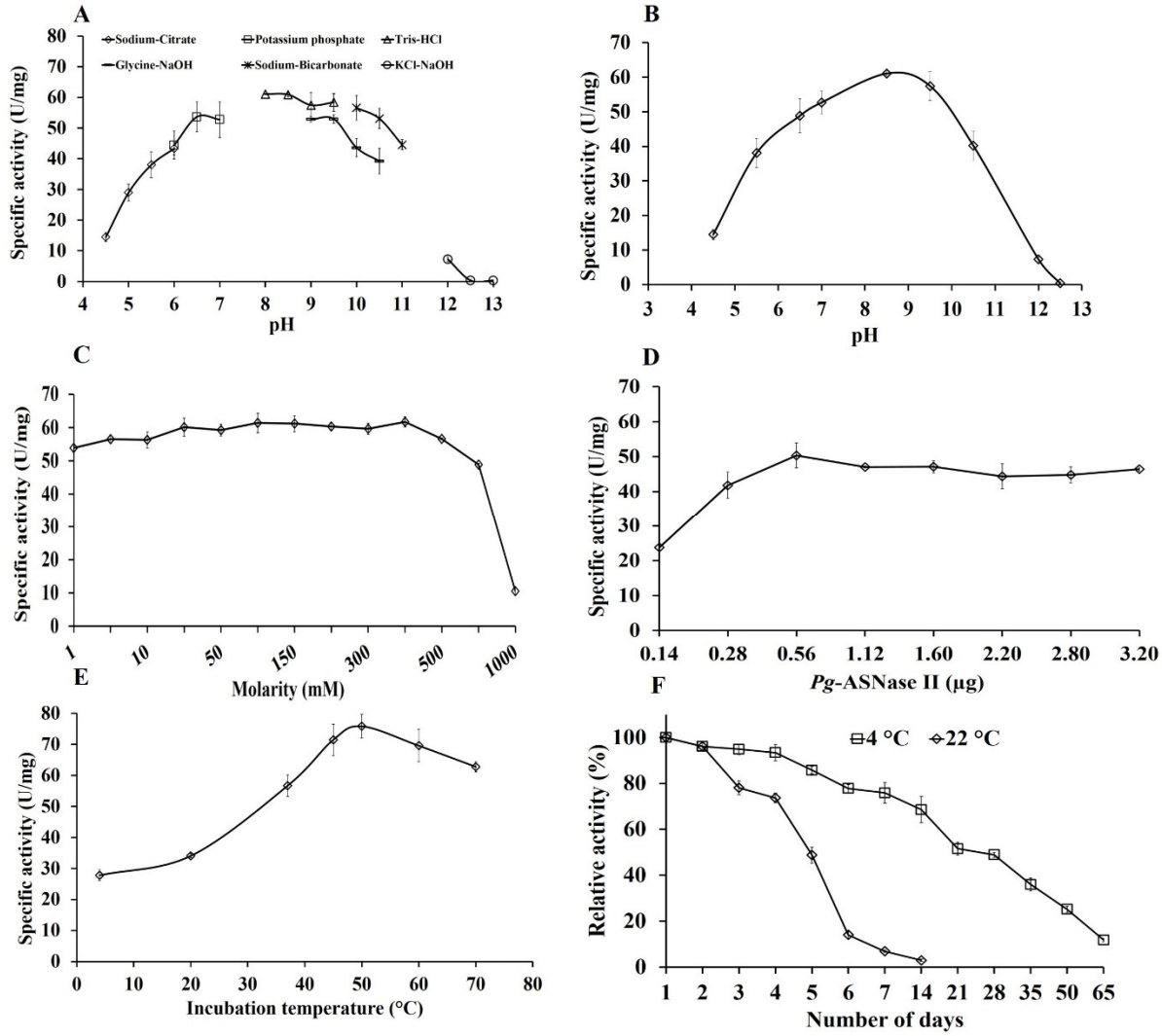

Figure 3. Optimization of different reaction parameters for His-tagged *Pg*-ASNase II. (**A**) Buffer, (**B**) pH, (**C**) Buffer molarity, (**D**) Enzyme concentration, (**E**) Incubation temperature, and (**F**) Shelf-life of *Pg*-ASNase II stored at 4 and 22 °C. The error bars represent the standard deviation of three experiments.

The enzyme retained 79.8 and 70% of original activity at 37 and 50 °C after 60 min, respectively. At higher temperatures, enzyme activity dropped rapidly and retained 40.13, 22.80, and 15.17% activity after 20 min incubation at 60, 70, and 80 °C, respectively (Figure 4). The half-life of *Pg*-ASNase II was measured to be 625.15 min at 37 °C with a dissociation constant (k_d) of 1.10′10^{-3} min (Table 2).

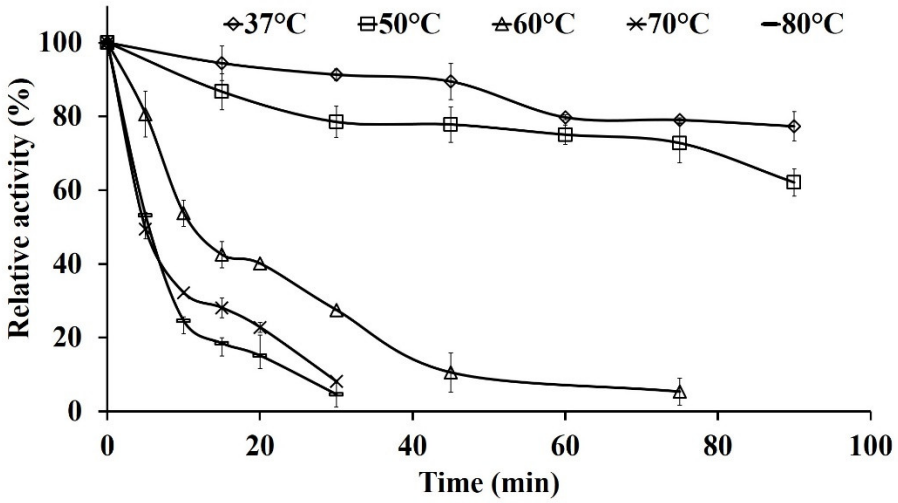

Figure 4. Thermostability assessment of His-tagged *Pg*-ASNase II. The thermostability of *Pg*-ASNase II was studied by incubating at 37–80 °C temperatures for 90 min in Tris-HCl buffer (50.0 mM and 8.5 pH), and the residual *Pg*-ASNase II activity was calculated. The error bars represent the standard deviation of three experiments.

Table 2. Half-life time ($t_{1/2}$) and heat deactivation constant (k_d) of *Pg*-ASNase II produced by *Pseudomonas* sp. PCH199.

Temperature (°C)	Half-Life (min)	k_d (min)	R^2 Value
37	625.15	1.10×10^{-3}	0.98
50	316.89	2.1×10^{-3}	0.96
60	46.77	14.8×10^{-3}	0.98
70	18.85	36.7×10^{-3}	0.95
80	17.86	38.8×10^{-3}	0.98

3.5. Effect of Metal Ions, Detergents, and Protein Modifier Agents

The effect of various metal ions, detergents, and protein modifying agents on the enzyme activity was analyzed. It was found that the metal ions Cu^{2+}, Zn^{2+}, K^{+}, Co^{2+}, Ca^{2+}, and Na^{+} had no significant effect on *Pg*-ASNase II activity. The enzyme activity remained unaffected by SDS at 2.0% concentration. Other detergents, such as Tween 20, Tween 80, and Triton X-100, showed precipitation in the enzyme reaction, which hindered enzyme activity measurements (Figure 5A). The protein modifiers EDTA, PMSF, and β-ME at 0.5 to 2.0 mM concentration did not affect the *Pg*-ASNase II activity. DTT at 1.0 mM concentration showed 14% inhibition, and above 1.0 mM precipitation was observed in the reaction (Figure 5B).

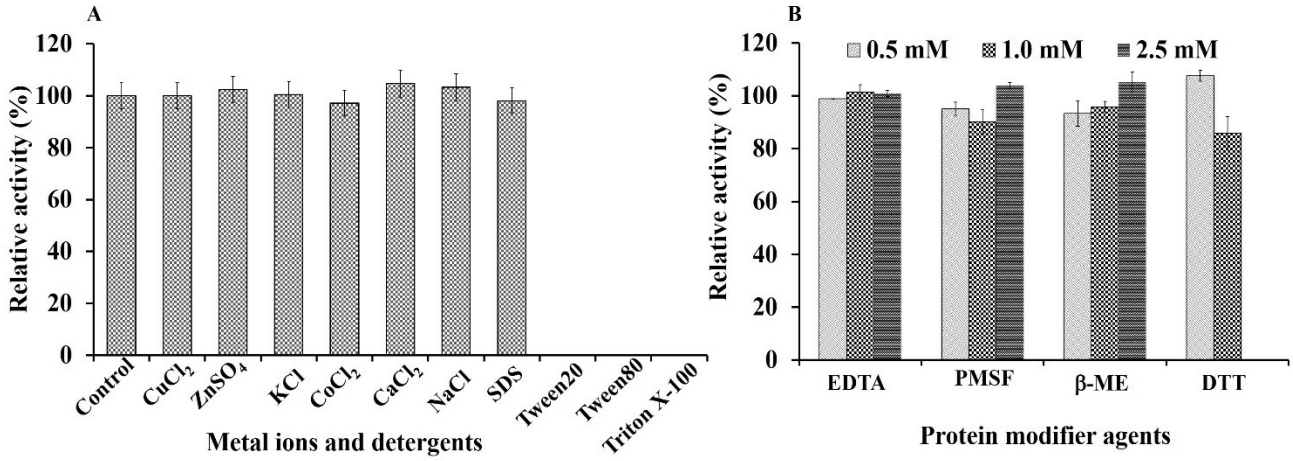

Figure 5. Effect of metal ions, detergents, and protein modifier agents on *Pg*-ASNase II activity. (**A**) The enzyme was incubated with 1.0 mM $CuCl_2$, $ZnSO_4$, KCl, $CoCl_2$, $CaCl_2$, and NaCl and 2.0% of SDS, Tween 20, Tween 80, and Triton X-100. The relative activity was calculated by considering the 100% activity of the enzyme without the addition of metal ions (control). (**B**) Protein modifier agents such as EDTA, PMSF, β-ME, and DTT were used at different concentrations of 0.5, 1.0, and 2.5 mM to assess the residual activity of *Pg*-ASNase II. The error bar represents the standard deviation of three experiments.

3.6. Enzyme Kinetics of Pg-ASNase II

The kinetics of his-tagged purified *Pg*-ASNase II was studied in optimal assay conditions, with varying concentrations of L-asparagine (0.1 to 5.0 mM). The K_m, V_{max}, k_{cat}, and k_{cat}/K_m values of recombinant *Pg*-ASNase II were determined to be 0.571 ± 0.06 μM, 71.42 ± 7.28 U/mg, 43.34 ± 4.49 s^{-1}, and 77.90 ± 9.81 s^{-1} mM^{-1} respectively (Figure 6A,B).

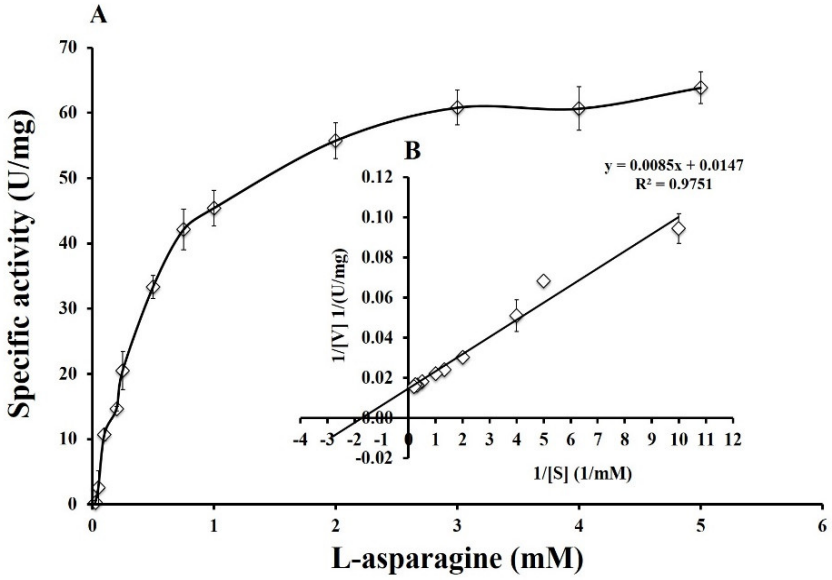

Figure 6. Kinetic study of His-tagged *Pg*-ASNase II. (**A**) Effect of varying L-asparagine concentration (0.10–5.0 mM) on *Pg*-ASNase II activity. (**B**) Lineweaver-Burk plot for determining a kinetic parameter of *Pg*-ASNase II for L-asparagine. The error bar represents the standard error of three experiments.

3.7. Anti-Proliferation Studies

The purified *Pg*-ASNase II exhibited cytotoxicity against cancer cell-line with increasing concentrations. The sensitivity of MCF-7 cells to *Pg*-ASNase II (tag-free) showed dose-dependency with significantly decreased cell survival compared to the control. The IC_{50} value was estimated to be 0.169 U/mL after 24 h of incubation (Figure 7A,B).

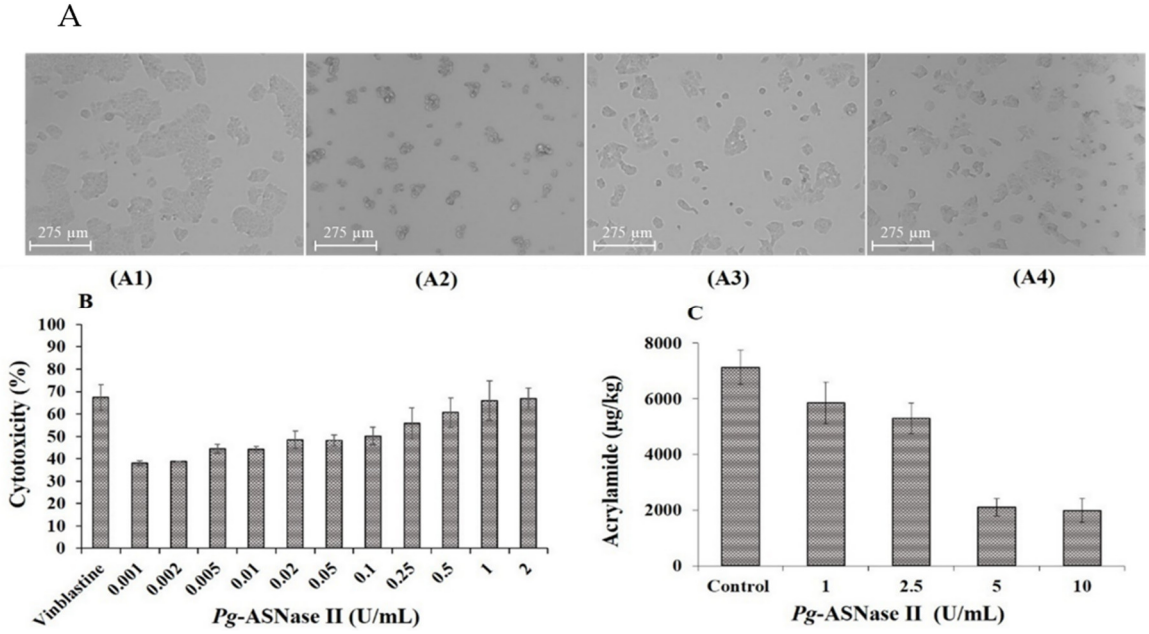

Figure 7. Exploration of the potential application of tag-free *Pg*-ASNase II. (**A**) Cytotoxicity against MCF-7 cells was tested using an MTT assay. (**A1**) control, (**A2**) vinblastine, (**A3**) effect of asparaginase in 24 h, and (**A4**) effect of *Pg*-ASNase II in 48 h. (**B**) Cytotoxic effect of purified tag-free *Pg*-ASNase II against MCF-7 breast cancer cell line when treated with varying enzyme concentrations. The cells were incubated for 24 h with purified enzyme, and cell viability was measured and compared with untreated cells. (**C**) Acrylamide content in fried potato chips treated with different doses of *Pg*-ASNase II prior to frying compared with untreated fried potato chips (control). The error bars represent the standard deviation of three experiments.

3.8. Acrylamide Reduction

Acrylamide content was calculated as 7131 µg/kg in the control sample, while 2108 µg/kg in treated potato samples with 5.0 U/mL *Pg*-ASNase II. It was seen that an approximately equal reduction in acrylamide content was recorded when 10.0 U/mL of *Pg*-ASNase II was used, corresponding to 2200 µg/kg of acrylamide content. Overall, the pretreated potato slices with 1.0, 2.5, 5.0, and 10.0 U/mL of *Pg*-ASNase II resulted in 17–70% acrylamide reduction in fried potatoes (Figure 7C, Table S2).

4. Discussion

L-ASNase is well known for its therapeutic ability to treat ALL and its application in reducing acrylamide in fried food. Exploring and finding new L-ASNase with effective antineoplastic activity and compatibility with the physiological environment of human blood has piqued the interest of researchers. The primary goal of this study was to evaluate the potential of recombinant L-ASNase II of *Pseudomonas* sp. PCH199 is a therapeutic candidate for antitumor applications and acrylamide reduction in the food industry.

4.1. In-Silico Analysis, Expression, and Purification of Pg-ASNase II

Based on a BLASTp UniProtKB/SwissProt homology search results, the isolated enzyme shared maximum identity with type II L-ASNase of *P. fluorescens* bv. The two signature sequences of *Pg*-ASNase II were identified as having Thr21 and Thr101 as active

site residues. Similarly, two signature sequences and Thr as a catalytic site residue have been reported in various type II L-ASNase such as *Pseudomonas* sp. PCH44, *C. amphilecti* AMI6, and *P. furiosus* [21,29,30]. Based on modeling, the *Pg*-ASNase II was predicted as homotetrameric (Figure S7). These results coincided with previous studies indicating a tetrameric configuration of several bacterial L-ASNases [6,21,31].

The cloning and expression of *Pg-asn* II were successfully done in *E. coli* BL21(DE3), followed by optimization of critical parameters influencing *Pg*-ASNase II production. The maximum expression of *Pg*-ASNase II was obtained in a lower IPTG (0.3 mM) concentration, an essential factor affecting gene expression. It directly influences overall cost, productivity, protein yield per cell, protein folding, and potential inhibitory effect on cell growth [32]. Similarly, the expression of L-ASNase from *Vibrio cholerae* (*V. cholerae*) [33] was maximum after 0.3 mM IPTG induction. After IPTG induction, the maximum production of *Pg*-ASNase II was optimized at 37 °C and 250 RPM. Similarly, *E. carotovora* [10] and *P. fluorescens* [34] L-ASNase exhibited optimum expression at 37 °C. The optimum agitation rate for L-ASNase production was 250 RPM for *Lactobacillus salivarius* (*L. salivarius*) [35].

The single-step purification of *Pg*-ASNase II yielded high protein using HisPur Cobalt Super-flow affinity chromatography and a Q-sepharose anion exchange chromatographic column. The molecular weight of the monomeric *Pg*-ASNase II was determined to be approximately 37.0 kDa using SDS-PAGE. Similarly, the molecular weight of a previously described L-ASNase produced from *Cobetia amphilecti* AMI6 (*C. amphilecti*), *E. coli*, and *Aliivibrio fischeri* (*A. fischeri*) was 37.0 kDa [29,36,37]. Type II L-ASNases have molecular weights varying from 31.0 to 42.0 kDa [21,33,37–39]. However, the purified L-ASNase from *Enterobacter cloacae* (*E. cloacae*) and *Streptomyces fradiae* NEAE-82 (*S. fradiae*) had a molecular weight of 52.0 and 53.0 kDa, respectively [40,41]. The native molecular weight of *Pg*-ASNase II was 148.0 kDa as determined by gel exclusion chromatography. Indicating that it is tetrameric, as predicted by the *in-silico* analysis. Similarly, type II L-ASNase from *E. chrysanthemi*, *Pseudomonas* sp. PCH44, *P. carotovorum,* and *E. coli,* are tetrameric forms [6,21,31,36]. Most type II L-ASNase derived from microbial sources has a tetrameric structure. However, many of the bacterial L-ASNase observed to be monomers, such as *Paenibaeillus barengoltzii* CAU904 (*P. barengoltzii*) [42], and homodimers in their native form, such as *Anoxybacillus flavithermus* (*A. flavithermus*) and *Bacillus cereus* BDRDST26 (*B. cereus*) [43,44].

4.2. Effect of Reaction Conditions and Kinetic Behavior of Pg-ASNase II

The purified *Pg*-ASNase II exhibited activity between pH 4.5–12.0 with optimum activity at pH 8.5. It indicated that *Pg*-ASNase II works best at a slightly alkaline pH, comparable to human blood pH. Similarly, L-ASNase of *E. coli* K-12 [36], *P. barengoltzii* [42], and *Geobacillus kaustophilus* DSM7263 (*G. kaustophilus*) [45] were reported for its maximum activity at pH 8.5. The *Pg*-ASNase II is active over a wide pH and could also be used for acrylamide mitigation in fried food. The optimum reaction temperature for recombinant *Pg*-ASNase II was 50 °C. As a result, *Pg*-ASNase II may be suitable for industrial applications requiring harsh conditions such as high-temperature exposure. These findings were consistent with that reported for L-ASNase of *B. cereus* BDRD-ST26 [44]. The optimum temperature for L-ASNase activity from *C. amphilecti* AMI6 [29], *D. chrysanthemi* [38], *P. barengoltzii* [42], *G. kaustophilus* DSM7263 [45], *Helicobacter pylori* (*H. pylori*) [46], *B. subtilis* [47], and *Burkholderia pseudomallei* (*B. pseudomallei*) [48] ranged from 37 to 60 °C. The key obstacles in the rapid development of biocatalyst-based processes are enzyme stability and thermal deactivation. Furthermore, it is considered an essential parameter of enzyme selection for industrial applications.

The thermostability profile of *Pg*-ASNase II shows that it retained 79.8 and 70% activity at 37 and 50 °C, respectively, when incubated for 60 min. The stability of the *Pg*-ASNase II at 37 °C (human body temperature) and 50 °C can be helpful in the therapeutic and food industries, respectively. *Pg*-ASNase II was more stable at 50 °C than previously

reported L-ASNase from *H. pylori*, which retained 50% activity after 36 min [46]. Similarly, L-ASNase from *V. cholerae* and *Bacillus sonorensis* retained only 2.0 and 22.8% activity, respectively [33,49]. The L-ASNase produced from *P. furiosus* [30] and *Thermococcus kodakarensis* [50] showed high thermal stability. The *Pg*-ASNase II was stable at 37 and 50 °C for a longer time with a 625 and 136 min half-life, respectively. It was observed to be higher than the commercially available L-ASNases from *E. coli* and *Erwinia* having a half-life of 276 and 444 min, respectively [51,52]. However, the half-life of *V. cholerae* [33] and *A. flavithermus* [43] was reported higher (18.3 and 48 h) at 37 °C, respectively. On the other hand, *Pg*-ASNase II had a longer half-life and a lower deactivation constant at 50 °C compared to L-ASNase from *S. brollosae* NEAE-115 [53].

The metal ions such as $CuCl_2$, $ZnSO_4$, KCl, $CoCl_2$, $CaCl_2$, and NaCl did not significantly affect the *Pg*-ASNase II activity. It suggested that *Pg*-ASNase II is not a metalloprotein. Similarly, for *C. amphilecti* AMI6 L-ASNase, none of the reported metal ions significantly affect the enzyme activity [29]. However, the metal ions had an inhibitory effect on the L-ASNase activity of *V. cholerae, P. fluorescens*, *B. pseudomallei,* and *S. brollosae* NEAE-115 [33,34,48,53]. The inhibitory effect might be due to the sulfhydryl group(s) present around the catalytic site of enzymes [33,54]. The *Pg*-ASNase II amino acid sequence does not have cysteine residue, so it lacks sulfhydryl groups, generally inhibited by the presence of various divalent metal ions.

The complete loss of *Pg*-ASNase II activity was observed by detergents such as Tween 20, Tween 80, and Triton X-100 due to precipitation with reaction. The protein modifying agent, such as EDTA, did not significantly influence *Pg*-ASNase II activity. Similar observations were made for the EDTA effect on the L-ASNase of *Aquabacterium* sp. A7-Y and *B. cereus* [44,55]. However, L-ASNase from *P. barengoltzii* and *B. pseudomallei* were inhibited by EDTA [42,48]. Additionally, *Pg*-ASNase II activity was not substantially affected by using PMSF as a protease inhibitor. It was concluded that serine did not have a catalytic function in the enzymatic reaction. A similar observation was recorded for the L-ASNase of *B. tequilensis* PV9W [56]. On the contrary, PMSF reduced *V. cholerae* L-ASNase activity [33], indicating the role of a serine residue in the catalytic site. Similarly, β-ME does not exhibit any significant inhibition at 0.5, 1.0, and 2.5 mM concentrations, which indicates the absence of S-S bridges in protein structure. The sequence analysis revealed that the *Pg*-ASNase II has no cysteine group; thus, the β-ME did not affect enzyme activity. Similarly, the *P. furiosus* L-ASNase activity was not inhibited by the presence of β-ME [30].

The *Pg*-ASNase II exhibited high substrate affinity towards L-asparagine. The K_m value of the *Pg*-ASNase II was lower (0.571 mM) than the reported value for *C. amphilecti* AMI6, *A. fischeri*, and *B. cereus* BDRD-ST26 [29,37,44]. Although, it was higher than commercially L-ASNase from *E. coli* (0.058 mM) and *E. chrysanthemi* (0.015 mM), respectively [57]. The lower K_m value is helpful for therapeutic L-ASNases because the concentration of L-asparagine in the blood is ~50 μM [6].

4.3. Potential Applications of Pg-ASNase II

Breast cancer is most common in women and has a high mortality rate. *Pg*-ASNase II was efficiently cytotoxic against the MCF-7 breast cancer cell line (IC_{50} value 0.169 U/mL). The low IC_{50} value indicates potential drug development with a low dosage amount. L-ASNase from various sources has been tested against the MCF-7 cell line. Similarly, L-ASNase of *Streptomyces rochei* [58] and *Bacillus velezensis* [59] were reported to inhibit the growth of the HeLa, HepG2, MDA-MB-231, and MCF-7 cell lines. Besides that, *Pg*-ASNase II showed a 70% reduction in acrylamide when treated with 5.0 U of the enzyme before frying. In an earlier study, L-ASNase from *B. cereus* BDRD-ST26 reduced acrylamide in potato slices by 72% compared to an untreated control [44]. Similarly, the L-ASNase of *C. amphilecti* AMI6 and *Bacillus subtilis* reduced 81 and 90% of acrylamide, respectively [55,60]. The complete reduction of acrylamide is not achievable due to the alternative pathways for acrylamide synthesis that are not directly dependent on L-asparagine [61].

The findings suggested that *Pg*-ASNase II could be employed effectively in the food industry. Furthermore, *Pseudomonas* sp. PCH199 represents a new perspective on bacterial resources for a stable L-ASNase having commercial applications.

5. Conclusions

In the present study, a type II L-ASNase of strain PCH199 was successfully cloned and expressed in *E. coli* BL21(DE3). The homotetrameric *Pg*-ASNase II exhibited high specific activity towards L-asparagine in Tris-HCl buffer (pH 8.5). The optimum temperature for *Pg*-ASNase II activity was 50 °C, and it was stable in the presence of various metal ions and protein modifying agents (EDTA, PMSF, and β-ME). The biochemical properties of the enzyme, such as optimal pH, buffer molarity, and temperature, demonstrated that *Pg*-ASNase II mimics physiological conditions similar to human blood. The cytotoxicity of *Pg*-ASNase II against the breast cell line MCF-7, and its ability of acrylamide reduction in potato slices, suggested its potential in both the pharmaceutical and food industries. Future research aims to reduce its K_m value using protein engineering methods that could make it a more viable chemotherapeutic drug in the biopharmaceutical industry.

Supplementary Materials: The following supporting information can be downloaded at: https://www.mdpi.com/article/10.3390/fermentation8100568/s1, Figure S1: Phylogenetic analysis of *Pg*-ASNase II proteins of *Pseudomonas* sp. PCH199. Based on an amino acid sequence alignment of L-ASNases proteins, a rooted phylogenetic tree was constructed with the NGPhylogeny.fr and annotated using the iTOL program. The scale bar corresponds to 0.1 amino acid change per site. The UniProt ID of all sequences is indicated in parentheses; Figure S2: Expression of *Pg*-ASNase II in LB media. (**a**) *Pg*-ASNase II (U/mL) activity and cell OD_{600} of recombinant *E. coli* BL21(DE3) after 6 h of induction with 0.5 mM IPTG. (**b**) Expression of recombinant colonies at 3 and 6 h of incubation at 37 °C in 12% SDS-PAGE; Figure S3: Expression of *Pg*-ASNase II in *E. coli* BL21(DE3) at different IPTG concentrations. Enzyme activity (U/mL) of recombinant *E. coli* BL21(DE3) in LB medium using 0.1 to 1.0 mM IPTG concentration and 12% SDS-PAGE analysis profiles of *Pg*-ASNase II expressed at different IPTG concentration for 0.0 and 5.0 h after induction; Figure S4: Production profile of *Pg*-ASNase II by recombinant *E. coli* grown in LB medium. (**a**) Effect of different levels of incubation temperature on the production of *Pg*-ASNase II activity after 5, 10, and 20 h of incubation at 20, 28, and 37 °C. (**b**) Effect of agitation on the *Pg*-ASNase II activity. (**c**) Effect of growth stages for IPTG induction on *Pg*-ASNase II activity. (**d**) A positive correlation between cell growth (line) and enzyme activity (bar chart) was observed. All the values are the means of three replicates ± SD; Figure S5: Optimizing the active soluble protein yield. (**a**) IPTG concentration (**b**) Incubation temperature after induction (**c**) Post induction time; Figure S6: Polyacrylamide gel electrophoresis of *Pg*-ASNase II. 10% SDS-PAGE of purified *Pg*-ASNase II elutions. Lane 1, Total lysate (TL); Lane 2, Flow through (FT); lane 3-9, different elutions (E1-E7) of purified Pg-ASNase II; and Lane M, molecular marker; Figure S7: Structure depiction of *Pg*-ASNase II using Swiss Model. Chain A; Blue colour, Chain B; Cyan colour, Chain C; yellow colour, Chain D; Red colour. Structural depiction of monomeric L-ASNase showing two domains, N-terminal and C-terminal for *Pg*-ASNase II; Table S1: The percentage identity matrix of similarities among five L-ASNase protein sequences with Pg-ASNase II sequence; Table S2: Acrylamide quantification in raw sample and reduction measures with different enzyme dosages.

Author Contributions: S.K.: Methodology, investigation, data curation, formal analysis, writing-original draft preparation. S.D.: Methodology, investigation, data curation, writing-original draft preparation. V.P.: Formal analysis, data curation. V.K.: Formal analysis, data curation. D.S.: Conceptualization, methodology, formal analysis, supervision, resources, visualization, writing-review, and editing. All authors have read and agreed to the published version of the manuscript.

Funding: Indian Council of Medical Research (ICMR), New Delhi, is duly acknowledged for financial support in the form of a Research Fellowship to S.K. (3/1/3/JRF-2016/HRD) and V.P. (5/3/8/26/ITR-F/2019-ITR), and a Young Scientist award to V.K. (R.12014/25/2020-HR). S.D. (20/12/2015(ii)EU-V) duly acknowledges fellowship support from the Council of Scientific and Industrial Research (CSIR), New Delhi. D.S. gratefully acknowledges financial support from CSIR, New Delhi, for research grants MLP0125 and 130.

Institutional Review Board Statement: Authors have not used humans or animals for conducting experiments in the present studies.

Informed Consent Statement: Not applicable.

Data Availability Statement: Whole-genome sequence of *Pseudomonas* sp. PCH199 (Project ID: PRJNA668072, Biosample ID: SAMN16396550) was submitted to the NCBI GenBank database and will be available publically after 9 October 2022.

Acknowledgments: Y.S. Padwad for extending animal cell culture support. Palampur is duly acknowledged for providing the necessary facility to carry out the work. This manuscript represents CSIR-IHBT publication number 5159.

Conflicts of Interest: The authors declare no conflict of interest.

References

1. Li, X.; Zhang, X.; Xu, S.; Xu, M.; Yang, T.; Wang, L.; Zhang, H.; Fang, H.; Osire, T.; Rao, Z. Insight into the thermostability of thermophilic L-asparaginase and non-thermophilic L-asparaginase II through bioinformatics and structural analysis. *Appl. Microbiol. Biotechnol.* **2019**, *103*, 7055–7070. https://doi.org/10.1007/S00253-019-09967-W/FIGURES/7.
2. Kelo, E.; Noronkoski, T.; Mononen, I. Depletion of L-asparagine supply and apoptosis of leukemia cells induced by human glycosylasparaginase. *Leukemia* **2009**, *23*, 1167–1171. https://doi.org/10.1038/leu.2008.387.
3. Chiu, M.; Taurino, G.; Bianchi, M.G.; Kilberg, M.S.; Bussolati, O. Asparagine synthetase in cancer: Beyond acute lymphoblastic leukemia. *Front. Oncol.* **2020**, *9*, 1480. https://doi.org/10.3389/fonc.2019.01480.
4. Michalska, K.; Jaskolski, M. Structural aspects of L-asparaginases, their friends and relations. *Acta Biochim. Pol.* **2006**, *53*, 627–640. https://doi.org/10.18388/abp.2006_3291.
5. Yun, M.K.; Nourse, A.; White, S.W.; Rock, C.O.; Heath, R.J. Crystal structure and allosteric regulation of the cytoplasmic *Escherichia coli* L-asparaginase I. *J. Mol. Biol.* **2007**, *369*, 794–811. https://doi.org/10.1016/j.jmb.2007.03.061.
6. Schalk, A.M.; Nguyen, H.A.; Rigouin, C.; Lavie, A. Identification and structural analysis of an L-asparaginase enzyme from guinea pig with putative tumor cell killing properties. *J. Biol. Chem.* **2014**, *289*, 33175–33186. https://doi.org/10.1074/jbc.M114.609552.
7. Covini, D.; Tardito, S.; Bussolati, O.; Chiarelli, L.R.; Pasquetto, M.V.; Digilio, R.; Valentini, G.; Scotti, C. Expanding targets for a metabolic therapy of cancer: L-asparaginase. *Recent Pat. Anticancer Drug Discov.* **2012**, *7*, 4–13. https://doi.org/10.2174/157489212798358001.
8. Baskar, G.; Lalitha, K.; Aiswarya, R.; Naveenkumar, R. Synthesis, characterization and synergistic activity of cerium-selenium nanobiocomposite of fungal L-asparaginase against lung cancer. *Mater. Sci. Eng. C* **2018**, *93*, 809–815. https://doi.org/10.1016/j.msec.2018.08.051.
9. Knott, S.R.; Wagenblast, E.; Khan, S.; Kim, S.Y.; Soto, M.; Wagner, M.; Turgeon, M.O.; Fish, L.; Erard, N.; Gable, A.L.; et al. Asparagine bioavailability governs metastasis in a model of breast cancer. *Nature* **2018**, *554*, 378–381. https://doi.org/10.1038/nature25465.
10. Kotzia, G.A.; Labrou, N.E. L-Asparaginase from *Erwinia chrysanthemi* 3937: Cloning, expression and characterization. *J. Biotechnol.* **2007**, *127*, 657–669. https://doi.org/10.1016/j.jbiotec.2006.07.037.
11. Horvat, T.Z.; Pecoraro, J.J.; Daley, R.J.; Buie, L.W.; King, A.C.; Rampal, R.K.; Tallman, M.S.; Park, J.H.; Douer, D. The use of *Erwinia* asparaginase for adult patients with acute lymphoblastic leukemia after pegaspargase intolerance. *Leuk. Res.* **2016**, *50*, 17–20. https://doi.org/10.1016/j.leukres.2016.08.014.
12. Fonseca, M.H.; da Silva Fiúza, T.; de Morais, S.B.; Trevizani, R. Circumventing the side effects of L-asparaginase. *Biomed. Pharmacother.* **2021**, *139*, 111616. https://doi.org/10.1016/j.biopha.2021.111616.
13. Jia, R.; Wan, X.; Geng, X.; Xue, D.; Xie, Z.; Chen, C. Microbial L-asparaginase for application in acrylamide mitigation from food: Current research status and future perspectives. *Microorganisms* **2021**, *9*, 1659. https://doi.org/10.3390/microorganisms9081659.
14. Mottram, D.S.; Wedzicha, B.L.; Dodson, A.T. Acrylamide is formed in the Maillard reaction. *Nature* **2002**, *419*, 448–449. https://doi.org/10.1038/419448a.
15. Rifai, L.; Saleh, F.A. A review on acrylamide in food: Occurrence, toxicity, and mitigation strategies. *Int. J. Toxicol.* **2020**, *39*, 93–102. https://doi.org/10.1177%2F1091581820902405.
16. Da Cunha, M.C.; dos Santos Aguilar, J.G.; de Melo, R.R.; Nagamatsu, S.T.; Ali, F.; de Castro, R.J.S.; Sato, H.H. Fungal L-asparaginase: Strategies for production and food applications. *Food Res. Int.* **2019**, *126*, 108658. https://doi.org/10.1016/J.FOODRES.2019.108658.
17. Kumar, V.; Thakur, V.; Ambika, K.S.; Singh, D. Bioplastic reservoir of diverse bacterial communities revealed along altitude gradient of Pangi-Chamba trans-Himalayan region. *FEMS Microbiol. Lett.* **2018**, *365*, 144. https://doi.org/10.1093/FEMSLE/FNY144.
18. Kumar, V.; Thakur, V.; Kumar, V.; Kumar, R.; Singh, D. Genomic insights revealed physiological diversity and industrial potential for *Glaciimonas* sp. PCH181 isolated from Satrundi glacier in Pangi-Chamba Himalaya. *Genomics* **2020**, *112*, 637–646. https://doi.org/10.1016/j.ygeno.2019.04.016.

19. Kumar, V.; Kumar, S.; Singh, D. Metagenomic insights into Himalayan glacial and kettle lake sediments revealed microbial community structure, function, and stress adaptation strategies. *Extremophiles* **2022**, *26*, 3. https://doi.org/10.1007/s00792-021-01252-x.
20. Kumar, V.; Kumar, S.; Darnal, S.; Patial, V.; Singh, A.; Thakur, V.; Kumar, S.; Singh, D. Optimized chromogenic dyes-based identification and quantitative evaluation of bacterial L-asparaginase with low/no glutaminase activity bioprospected from pristine niches in Indian trans-Himalaya. *3 Biotech* **2019**, *9*, 275. https://doi.org/10.1007/s13205-019-1810-9.
21. Kumar, S.; Darnal, S.; Patial, V.; Kumar, V.; Kumar, V.; Kumar, S.; Singh, D. Molecular cloning, characterization, and in-silico analysis of l-asparaginase from Himalayan *Pseudomonas* sp. PCH44. *3 Biotech* **2022**, *12*, 162. https://doi.org/10.1007/s13205-022-03224-0.
22. Patial, V.; Kumar, V.; Joshi, R.; Gupta, M.; Singh, D. Acrylamide mitigation in foods using recombinant L-asparaginase: An extremozyme from Himalayan *Pseudomonas* sp. PCH182. *Food Res. Int*. **2022**, *162*, 111936. https://doi.org/10.1016/j.foodres.2022.111936.
23. Almagro Armenteros, J.J.; Tsirigos, K.D.; Sonderby, C.K.; Petersen, T.N.; Winther, O.; Brunak, S.; von Heijne, G.; Nielsen, H. SignalP 5.0 improves signal peptide predictions using deep neural networks. *Nat. Biotechnol*. **2019**, *37*, 420–423. https://doi.org/10.1038/s41587-019-0036-z.
24. Robert, X.; Gouet, P. Deciphering key features in protein structures with the new ENDscript server. *Nucleic Acids Res.* **2014**, *42*, W320–W324. https://doi.org/10.1093/nar/gku316.
25. Bergmans, H.E.N.; van Die, I.M.; Hoekstra, W.P.M. Transformation in *Escherichia coli*: Stages in the process. *J. Bacteriol*. **1981**, *146*, 564–570. https://doi.org/10.1128/JB.146.2.564-570.1981.
26. Laemmli, U.K. Cleavage of Structural Proteins during the Assembly of the Head of Bacteriophage T4. *Nature* **1970**, *227*, 680–685. https://doi.org/10.1038/227680a0.
27. Imada, A.; Igarasi, S.; Nakahama, K.; Isono, M. Asparaginase and glutaminase activities of microorganisms. *J. Gen. Microbiol.* **1973**, *76*, 85–99. https://doi.org/10.1099/00221287-76-1-85/CITE/REFWORKS.
28. Paleologos, E.K.; Kontominas, M.G. Determination of acrylamide and methacrylamide by normal phase high performance liquid chromatography and UV detection. *J. Chromatogr. A* **2005**, *1077*, 128–135. https://doi.org/10.1016/j.chroma.2005.04.037.
29. Farahat, M.G.; Amr, D.; Galal, A. Molecular cloning, structural modeling and characterization of a novel glutaminase-free L-asparaginase from *Cobetia amphilecti* AMI6. *Int. J. Biol. Macromol.* **2020**, *143*, 685–695. https://doi.org/10.1016/j.ijbiomac.2019.10.258.
30. Saeed, H.; Hemida, A.; El-Nikhely, N.; Abdel-Fattah, M.; Shalaby, M.; Hussein, A.; Eldoksh, A.; Ataya, F.; Aly, N.; Labrou, N.; et al. Highly efficient *Pyrococcus furiosus* recombinant L-asparaginase with no glutaminase activity: Expression, purification, functional characterization, and cytotoxicity on THP-1, A549 and Caco-2 cell lines. *Int. J. Biol. Macromol.* **2020**, *156*, 812–828. https://doi.org/10.1016/j.ijbiomac.2020.04.080.
31. Lubkowski, J.; Wlodawer, A. Structural and biochemical properties of L-asparaginase. *FEBS J.* **2021**, *288*, 4183–4209. https://doi.org/10.1111/FEBS.16042.
32. Silaban, S.; Gaffar, S.; Simorangkir, M.; Maksum, I.P.; Subroto, T. Effect of IPTG concentration on recombinant human prethrombin-2 expression in *Escherichia coli* BL21(DE3) ArcticExpress. *IOP Conf. Ser. Earth Environ. Sci.* **2018**, *217*, 012039. https://doi.org/10.1088/1755-1315/217/1/012039.
33. Radha, R.; Arumugam, N.; Gummadi, S.N. Glutaminase free L-asparaginase from *Vibrio cholerae*: Heterologous expression, purification and biochemical characterization. *Int. J. Biol. Macromol.* **2018**, *111*, 129–138. https://doi.org/10.1016/j.ijbiomac.2017.12.165.
34. Sindhu, R.; Manonmani, H.K. Expression and characterization of recombinant l-asparaginase from *Pseudomonas fluorescens*. *Protein Expr. Purif.* **2018**, *143*, 83–91. https://doi.org/10.1016/j.pep.2017.09.009.
35. Bhargavi, M.; Jayamadhuri, R. Isolation and screening of marine bacteria producing anti-cancer enzyme L-asparaginase. *Am. J. Mar. Sci.* **2016**, *4*, 1–3. https://doi.org/10.12691/marine-4-1-1.
36. Upadhyay, A.K.; Singh, A.; Mukherjee, K.J.; Panda, A.K. Refolding and purification of recombinant L-asparaginase from inclusion bodies of *E. coli* into active tetrameric protein. *Front. Microbiol.* **2014**, *5*, 486. https://doi.org/10.3389/fmicb.2014.00486.
37. Bento, H.; Paiva, G.B.; Almeida, M.R.; Silva, C.G.; Carvalho, P.J.; Tavares, A.P.; Pedrolli, D.B.; Santos-Ebinuma, V.C. *Aliivibrio fischeri* L-Asparaginase production by engineered *Bacillus subtilis*: A potential new biopharmaceutical. *Bioprocess. Biosyst. Eng*. **2022**, *45*, 1635–1644. https://doi.org/10.1007/s00449-022-02769-x.
38. Saeed, H.; Elsawy, E.; Shalaby, M.; Abdel-Fattah, M.; Hemida, A.; Eldoksh, A.; Ataya, F.S.; Nematalla, H.; Elkewedi, M.; Labrou, N.N.; et al. L-asparaginase from *Dickeya chrysanthemi*: Expression, purification and cytotoxicity assessment. *Prep. Biochem. Biotechnol.* **2022**, *52*, 668–680. https://doi.org/10.1080/10826068.2021.1983831.
39. Lee, S.J.; Lee, Y.; Park, G.H.; Umasuthan, N.; Heo, S.J.; de Zoysa, M.; Jung, W.K.; Lee, D.W.; Kim, H.; Kang, D.H.; et al. A newly identified glutaminase-free L-asparaginase (L-ASPG86) from the marine bacterium *Mesoflavibacter zeaxanthinifaciens*. *J. Microbiol. Biotechnol.* **2016**, *26*, 1115–1123. https://doi.org/10.4014/jmb.1510.10092.
40. El-Naggar, N.E.A.; Deraz, S.F.; Soliman, H.M.; El-Deeb, N.M.; El-Ewasy, S.M. Purification, characterization, cytotoxicity and anticancer activities of L-asparaginase, anti-colon cancer protein, from the newly isolated alkaliphilic *Streptomyces fradiae* NEAE-82. *Sci. Rep.* **2016**, *6*, 32926. https://doi.org/10.1038/srep32926.

41. Husain, I.; Sharma, A.; Kumar, S.; Malik, F. Purification and characterization of glutaminase free asparaginase from *Enterobacter cloacae*: In-vitro evaluation of cytotoxic potential against human myeloid leukemia HL-60 cells. *PLoS ONE* **2016**, *11*, e0148877. https://doi.org/10.1371/JOURNAL.PONE.0148877.
42. Shi, R.; Liu, Y.; Mu, Q.; Jiang, Z.; Yang, S. Biochemical characterization of a novel L-asparaginase from *Paenibacillus barengoltzii* being suitable for acrylamide reduction in potato chips and mooncakes. *Int. J. Biol. Macromol.* **2017**, *96*, 93–99. https://doi.org/10.1016/j.ijbiomac.2016.11.115.
43. Maqsood, B.; Basit, A.; Khurshid, M.; Bashir, Q. Characterization of a thermostable, allosteric L-asparaginase from *Anoxybacillus flavithermus*. *Int. J. Biol. Macromol.* **2020**, *152*, 584–592. https://doi.org/10.1016/j.ijbiomac.2020.02.246.
44. Feng, Y.; Liu, S.; Jiao, Y.; Wang, Y.; Wang, M.; Du, G. Gene cloning and expression of the l-asparaginase from *Bacillus cereus* BDRD-ST26 in *Bacillus subtilis* WB600. *J. Biosci. Bioeng.* **2019**, *127*, 418–424. https://doi.org/10.1016/j.jbiosc.2018.09.007.
45. Özdemir, F.İ.; Orhan, M.D.; Atasavum, Z.; Tülek, A. Biochemical characterization and detection of antitumor activity of l-asparaginase from thermophilic *Geobacillus kaustophilus* DSM 7263T. *Protein Expr. Purif.* **2022**, *199*, 106146. https://doi.org/10.1016/j.pep.2022.106146.
46. Cappelletti, D.; Chiarelli, L.R.; Pasquetto, M.V.; Stivala, S.; Valentini, G.; Scotti, C. *Helicobacter pylori* L-asparaginase: A promising chemotherapeutic agent. *Biochem. Biophys. Res. Commun.* **2008**, *377*, 1222–1226. https://doi.org/10.1016/j.bbrc.2008.10.118.
47. Jia, M.; Xu, M.; He, B.; Rao, Z. Cloning, expression, and characterization of L-asparaginase from a newly isolated *Bacillus subtilis* B11–06. *J. Agric. Food Chem.* **2013**, *61*, 9428–9434. https://doi.org/10.1021/jf402636w.
48. Darwesh, D.B.; Al-Awthan, Y.S.; Elfaki, I.; Habib, S.A.; Alnour, T.M.; Darwish, A.B.; Youssef, M.M. Anticancer Activity of Extremely Effective Recombinant L-Asparaginase from *Burkholderia pseudomallei*. *J. Microbiol. Biotechnol.* **2022**, *32*, 551–563. https://doi.org/10.4014/jmb.2112.12050.
49. Aly, N.; El-Ahwany, A.; Ataya, F.S.; Saeed, H. *Bacillus sonorensis* L-asparaginase: Cloning, expression in *E. coli* and characterization. *Protein J.* **2020**, *39*, 717–729. https://doi.org/10.1007/S10930-020-09932-X.
50. Chohan, S.M.; Sajed, M.; un Naeem, S.; Rashid, N. Heterologous gene expression and characterization of TK2246, a highly active and thermostable plant type L-asparaginase from *Thermococcus kodakarensis*. *Int. J. Biol. Macromol.* **2020**, *147*, 131–137. https://doi.org/10.1016/j.ijbiomac.2020.01.012.
51. Zhang, J.F.; Shi, L.Y.; Wei, D.Z. Chemical modification of L-asparaginase from *Escherichia coli* with a modified polyethyleneglycol under substrate protection conditions. *Biotechnol. Lett.* **2004**, *26*, 753–756. https://doi.org/10.1023/B:BILE.0000024100.49716.3d.
52. Egler, R.A.; Ahuja, S.P.; Matloub, Y. L-asparaginase in the treatment of patients with acute lymphoblastic leukemia. *J. Pharmacol. Pharmacother.* **2016**, *7*, 62–71. https://doi.org/10.4103/0976-500X.184769.
53. El-Naggar, N.E.A.; Deraz, S.F.; El-Ewasy, S.M.; Suddek, G.M. Purification, characterization and immunogenicity assessment of glutaminase free L-asparaginase from *Streptomyces brollosae* NEAE-115. *BMC Pharmacol. Toxicol.* **2018**, *19*, 51. https://doi.org/10.1186/S40360-018-0242-1/TABLES/5.
54. Warangkar, S.C.; Khobragade, C.N. Purification, characterization, and effect of thiol compounds on activity of the *Erwinia carotovora* L-asparaginase. *Enzyme Res.* **2010**, *2010*, 165878. https://doi.org/10.4061/2010/165878.
55. Sun, Z.; Qin, R.; Li, D.; Ji, K.; Wang, T.; Cui, Z.; Huang, Y. A novel bacterial type II l-asparaginase and evaluation of its enzymatic acrylamide reduction in french fries. *Int. J. Biol. Macromol.* **2016**, *92*, 232–239. https://doi.org/10.1016/J.IJBIOMAC.2016.07.031.
56. Shakambari, G.; Birendranarayan, A.K.; Angelaa Lincy, M.J.; Rai, S.K.; Ahamed, Q.T.; Ashokkumar, B.; Saravanan, M.; Mahesh, A.; Varalakshmi, P.; Hemocompatible glutaminase free L-asparaginase from marine *Bacillus tequilensis* PV9W with anticancer potential modulating p53 expression. *RSC Adv.* **2016**, *6*, 25943–25951. https://doi.org/10.1039/C6RA00727A.
57. Narta, U.K.; Kanwar, S.S.; Azmi, W. Pharmacological and clinical evaluation of L-asparaginase in the treatment of leukemia. *Crit. Rev. Oncol. Hematol.* **2007**, *61*, 208–221. https://doi.org/10.1016/j.critrevonc.2006.07.009.
58. El-Naggar, N.E.A.; El-Shweihy, N.M. Bioprocess development for L-asparaginase production by *Streptomyces rochei*, purification and in-vitro efficacy against various human carcinoma cell lines. *Sci. Rep.* **2020**, *10*, 7942. https://doi.org/10.1038/s41598-020-64052-x.
59. Mostafa, Y.; Alrumman, S.; Alamri, S.; Hashem, M.; Al-izran, K.; Alfaifi, M.; Elbehairi, S.E.; Taha, T. Enhanced production of glutaminase-free l-asparaginase by marine *Bacillus velezensis* and cytotoxic activity against breast cancer cell lines. *Electron. J. Biotechnol.* **2019**, *42*, 6–15. https://doi.org/10.1016/J.EJBT.2019.10.001.
60. Onishi, Y.; Prihanto, A.A.; Yano, S.; Takagi, K.; Umekawa, M.; Wakayama, M. Effective treatment for suppression of acrylamide formation in fried potato chips using L-asparaginase from *Bacillus subtilis*. *3 Biotech* **2015**, *5*, 783–789. https://doi.org/10.1007/S13205-015-0278-5/FIGURES/5.
61. Baskar, G.; Aiswarya, R. Overview on mitigation of acrylamide in starchy fried and baked foods. *J. Sci. Food Agric.* **2018**, *98*, 4385–4394. https://doi.org/10.1002/jsfa.9013.